Inorg. Chem. **2007**, *46*, 6473–6482

Synthesis and Structural Properties of Lanthanide Complexes Formed with Tropolonate Ligands

Jian Zhang, Paul D. Badger, Steven J. Geib, and Stéphane Petoud*

Department of Chemistry, University of Pittsburgh, Pittsburgh, Pennsylvania 15260

Received March 20, 2007

We have previously reported the unique luminescence properties of ML_4 complexes formed between tropolonate ligands and a series of lanthanide cations, several of them emitting in the near-infrared domain. The synthesis and composition of ML_4 lanthanide tropolonate complexes have been previously described in the literature, but no structural information has been available so far. In this work, the crystal structures of several lanthanide tropolonate complexes (Ln^{3+} = Tb^{3+}, Dy^{3+}, Ho^{3+}, Er^{3+}, Tm^{3+}, Yb^{3+}, Lu^{3+}) have been isolated and systematically analyzed by X-ray diffraction and compared by using different criteria including the Kepert formalism. Such comparative work is rare in lanthanide coordination chemistry. The analysis of the structures in the solid state reveals that although the packing of the ML_4 complexes depends on the nature of the metal ion, the coordination geometries around the different lanthanides is virtually similar for all the cations that have been analyzed; an indication that lanthanide-centered f orbitals play a role in controlling this coordination geometry. Analysis of the solution's behavior by stability constant determination reveals the formation of complexes with similar ML_4 stoichiometries as those observed in the solid state. Nevertheless, analysis of the luminescence lifetimes indicates that the coordination environment around the lanthanide cations are different in the solid state and in solution, with the presence of one molecule of water bound to the lanthanide cation in solution. The presence of such a water molecule is a significant source of nonradiative deactivation of the excited states of the lanthanide cations, an unfavorable condition that leads to significant loss in fluorescence intensity of these lanthanide complexes. This exemplifies that such comparative analysis between the solid state and solution is important for the rationalization of the luminescence properties of the complexes. This analysis will aid us in optimizing ligand design for improved photophysical properties of the complex.

Introduction

Tropolone (2-hydroxycyclohepta-2,4,6-trienone) and its derivatives have been studied in various fields such as medicinal and material sciences because of their biological activities[1] and their ability to form metallomesogens,[2,3] respectively. Tropolone derivatives have also been used as dynamic molecular systems for intramolecular proton tunneling[4,5] and proton transfer due to their structural tautomerism.[6] All these properties result from the molecular and electronic structure of the tropolone, a seven-membered non-benzenoid aromatic ring compound. Its pKa value of 6.7[7] allows for complete deprotonation at physiological conditions. Like the benzenoid catecholato ligand,[8−10] tropolone is a versatile bidentate chelating agent, suitable as a chelating group for d-block and f-block metal ions.

In most tropolonate metal complexes, the deprotonated hydroxyl group and the carbonyl oxygen are involved in the coordination to the metal ion, resulting in a bidentate complex (Scheme 1). This forms a thermodynamically favored five-membered chelate ring. Muetterties et al. were among the first to study tropolonate lanthanide coordination com-

* To whom correspondence should be addressed. E-mail: spetoud@pitt.edu.

(1) Erdtman, H.; Gripenberg, J. *Nature* **1948**, *161*, 719.
(2) Chipperfield, J. R.; Clark, S.; Elliott, J.; Sinn, E. *Chem. Commun.* **1998**, 195.
(3) Elliott, J. M.; Chipperfield, J. R.; Clark, S.; Sinn, E. *Inorg. Chem.* **2002**, *41*, 293.
(4) Redington, R. L. *J. Chem. Phys.* **2000**, *113*, 2319.
(5) Tanaka, K.; Honjo, H.; Tanaka, T.; Kohguchi, H.; Ohshima, Y.; Endo, Y. *J. Chem. Phys.* **1999**, *110*, 1969.
(6) Tanaka, K.; Nagahiro, R.; Ohba, S.; Eishima, M. *Tetrahedron Lett.* **2001**, *42*, 925.
(7) Doering, W. v. E.; Knox, L. H. *J. Am. Chem. Soc.* **1951**, *73*, 828.
(8) Carey, G. H.; Martell, A. E. *J. Am. Chem. Soc.* **1967**, *89*, 2859.
(9) Pierpont, C. G.; Buchanan, R. M. *Coord. Chem. Rev.* **1981**, *38*, 45.
(10) Albrecht, M. *Chem. Soc. Rev.* **1998**, *27*, 281.

10.1021/ic7005343 CCC: $37.00
Published on Web 07/10/2007

Scheme 1

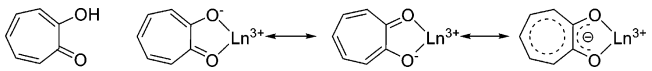

plexes.[11] They point out that tropolonate's compact shape, skeletal rigidity, and small bite angle make it a very suitable ligand for complexes with high coordination number. Using specific synthetic conditions, they were able to control the nature of two types of complexes (ML_3 and ML_4 formula). Three different types of counterions have been described for the ML_4 systems: Na^+, Li^+, and NH_4^+. The molecular formulas of these complexes were obtained from elemental analysis since it was a common technique available at that time. Information on the coordination geometry of the cation in these lanthanide complexes was not available since they had not been analyzed by X-ray crystallography.

One of the main reasons of our interest for tropolonate ligand for lanthanide coordination is its unique ability to sensitize several lanthanide cations emitting in the near-infrared (NIR) domain.[12−25] We have disclosed preliminary results describing mostly the photophysical properties of these tropolonate complexes in a communication.[26] Through the choice of the appropriate counterions and synthetic conditions, we were able to reproducibly prepare complexes with the ML_4 stoichiometry, and for the first time, the structure of seven different lanthanide complexes were isolated and analyzed. Through X-ray crystal analysis, we have been able to systematically compare the solid-state structures of these seven complexes. It is important to note that there are few reported examples of crystallographically characterized lanthanide complexes formed with the same ligand coordinating a series of lanthanide cations. The solid-state structural analysis was completed by the investigation of the complex species formed in solution through absorption spectrophotometric titrations, electrospray ionization mass spectroscopy, NMR, and luminescence techniques. The results of this investigation indicated that the coordination around the lanthanide cations are different in solution and in the solid state.

Experimental Section

Materials. All reagents were used as received, unless otherwise stated. Tropolone, $LnCl_3 \cdot nH_2O$ (Ln = La, Nd, Eu, Gd, Er, and Yb, 99.9% or 99.99%, $n = 6$ or 7), $YCl_3 \cdot 6H_2O$ (99.99%), and KOH standard solution in methanol (0.103 N) were purchased from Aldrich. $LnCl_3 \cdot nH_2O$ (Ln = Pr, Sm, Tb, Dy, Ho, Tm, and Lu, 99.9% or 99.99%, $n = 6$ or 7) were purchased from Strem Chemicals. All deuterated NMR solvents were purchased from Cambridge Isotope Labs and used as received.

Synthesis of Complexes and Preparation of Single Crystals. To a solution of tropolone (48.8 mg, 0.04 mmol) in MeOH (10 mL) was added KOH (0.04 mmol) in methanol (0.103 M) with stirring. To the resulting solution was added $LnCl_3 \cdot nH_2O$ (0.01 mmol) (Ln = La, Pr, Nd, Sm, Eu, Gd, Tb, Dy, Ho, Er, Tm, Yb, and Lu) or $YCl_3 \cdot 6H_2O$ in methanol (10 mL). The solution was stirred for 3 h, and the resulting precipitate was filtered, washed three times with methanol, and dried in vacuo over P_2O_5 for 48 h. Single crystals of $\{K[Ln(Trop)_4]DMF\}_\infty$ (Trop = $C_7H_5O_2^-$, tropolonate) were obtained from slow diffusion of diethyl ether into DMF solutions of $K[Ln(Trop)_4]$.

Methods. Infrared spectra were recorded on a Perkin-Elmer Spectrum BX FT-IR instrument. Elemental analyses were performed by Atlantic Microlab, Inc. (Norcross, GA). ^1H NMR spectra were recorded on a Bruker DPX-300 spectrometer at 300 MHz. MS-ESI were measured on an Agilent HP 1100 series LC-MSD instrument. UV−vis absorption spectra were recorded on a Perkin-Elmer Lambda 19 spectrophotometer.

Spectrophotometric Titrations. Spectrophotometric titrations were performed with a Perkin-Elmer Lambda 19 spectrophotometer connected to an external computer. All titrations were performed in a thermostated (25.0 ± 0.1 °C) cuvette in DMSO at constant ionic strength $\mu = 0.01$ M (tetrabutylammonium perchlorate). In a typical experiment, 2.00 mL of a ligand (potassium tropolonate) solution in DMSO (initial total ligand concentration 5×10^{-5} M) was titrated with lanthanide chloride solutions in DMSO (stock solution concentration: 1×10^{-4} M). After each addition of the lanthanide salt solution, the UV−vis spectrum the solution was measured. Factor analysis and mathematical treatment of the spectrophotometric data were performed with the SPECFIT program.[27]

Luminescence Measurements. The luminescence lifetime measurements were performed by excitation of solutions in 1 cm quartz cells using a nitrogen laser (Oriel model 79110, wavelength 337.1 nm, pulse width at half-height 15 ns, 5−30 Hz repetition rate). Emission from the sample was collected at a right angle to the excitation beam by a 3 in. plano-convex lens. Emission wavelengths were selected by means of quartz filters. The signal was monitored by a cooled photomultiplier (Hamamatsu R316) coupled to a 500 MHz bandpass digital oscilloscope (Tektronix TDS 754D). The signals (15 000 points each trace) from at least 500 flashes were collected and averaged. Background signals were similarly collected and subtracted from sample signals. Lifetimes are averages of at least three independent determinations. Data were fitted to exponential decay by Origin Pro (V7 SP4) data analysis software.

(11) Muetterties, E. L.; Wright, C. M. *J. Am. Chem. Soc.* **1965**, *87*, 4706.
(12) Bünzli, J.-C. G.; Piguet, C. *Chem. Soc. Rev.* **2005**, *34*, 1048.
(13) Bünzli, J.-C. G. *Acc. Chem. Res.* **2006**, *39*, 53.
(14) Aime, S.; Barge, A.; Batsanov, A. S.; Botta, M.; Castelli, D. D.; Fedeli, F.; Mortillaro, A.; Parker, D.; Puschmann, H. *Chem. Commun.* **2002**, 1120.
(15) Foley, T. J.; Harrison, B. S.; Knefely, A. S.; Abboud, K. A.; Reynolds, J. R.; Schanze, K. S.; Boncella, J. M. *Inorg. Chem.* **2003**, *42*, 5023.
(16) Quici, S.; Cavazzini, M.; Marzanni, G.; Accorsi, G.; Armaroli, N.; Ventura, B.; Barigelletti, F. *Inorg. Chem.* **2005**, *44*, 529.
(17) Torelli, S.; Imbert, D.; Cantuel, M.; Bernardinelli, G.; Delahaye, S.; Hauser, A.; Bünzli, J. -C. G.; Piguet, C. *Chem. Eur. J.* **2005**, *11*, 3228.
(18) Imbert, D.; Cantuel, M.; Bünzli, J.-C. G.; Bernardinelli, G.; Piguet, C. *J. Am. Chem. Soc.* **2003**, *125*, 15698.
(19) Pope, S. J. A.; Coe, B. J.; Faulkner, S.; Bichenkova, E. V.; Yu, X.; Douglas, K. T. *J. Am. Chem. Soc.* **2004**, *126*, 9490.
(20) Hebbink, G. A.; Grave, L.; Woldering, L. A.; Reinhoudt, D. N.; van Veggel, F. C. J. M. *J. Phys. Chem. A* **2003**, *107*, 2483.
(21) Pope, S. J. A.; Coe, B. J.; Faulkner, S.; Laye, R. H. *Dalton Trans.* **2005**, 1482.
(22) Davies, G. M.; Pope, S. J. A.; Adams, H.; Faulkner, S.; Ward, M. D. *Inorg. Chem.* **2005**, *44*, 4656.
(23) Van Deun, R.; Fias, P.; Nockemann, P.; Schepers, A.; Parac-Vogt, T. N.; Van Hecke, K.; Van Meervelt, L.; Binnemans, K. *Inorg. Chem.* **2004**, *43*, 8461.
(24) Lenaerts, P.; Driesen, K.; Van Deun, R.; Binnemans, K. *Chem. Mater.* **2005**, *17*, 2148.
(25) Bertolo, L.; Tamburini, S.; Vigato, P. A.; Porzio, W.; Macchi, G.; Meinardi, F. *Eur. J. Inorg. Chem.* **2006**, 2370.
(26) Zhang, J.; Badger, P. D.; Geib, S. J.; Petoud, S. *Angew. Chem., Int. Ed.* **2005**, *44*, 2508.
(27) Gampp, H.; Maeder, M.; Meyer, C. J.; Zuberbuehler, A. D. *Talanta* **1985**, *32*, 1133.

X-ray Crystallography. Crystals suitable for X-ray diffraction were coated with Fluorolube then mounted on a glass fiber and coated with epoxy cement. X-ray data were collected on a Bruker Apex diffractometer using graphite-monochromatized Mo Kα radiation ($\lambda = 0.71073$ Å). Data collection was controlled using the Bruker SMART program, and the data processing was completed with the SHELXTL program package. Graphical representations were obtained with the help of Ortep-3, Mercury 1.2.1, and Ortex software packages. All hydrogen atoms were calculated and placed in idealized positions ($d_{C-H} = 0.96$ Å).

Results and Discussion

Synthesis. The lanthanide complexes were synthesized in methanol using a 1:4 (metal/ligand) stoichiometry. Tropolone ligands were deprotonated by adding 1 equiv of KOH in methanol prior to addition of lanthanide chloride salt in the reaction mixture. Muetterties et al.[11] synthesized $[Ln(Trop)_4]^-$ complexes by reacting the $Ln(Trop)_3$ complex with NaTrop or LiTrop in a mixture of methanol and water. Our method is more straightforward and rapid: the total synthesis duration is 3 h, a significantly shorter time compared to the reaction time of the Muetterties method (15 h and 2 days for Na-$[Ln(Trop)_4]$ and Li$[Ln(Trop)_4]$, respectively) and leads to the isolation of the potassium salt, in comparison to the sodium and lithium salt for the Muetterties method. The difference in the nature of the counterion can have a significant role in the structures of the resultant complexes, as described recently the for rare-earth quinolinate system.[23] Although the same recrystallization method was systematically used for all the lanthanide tropolonate complexes, we were only able to isolate crystals suitable for X-ray diffraction for Tb^{3+} to Lu^{3+} but not for the larger lanthanide cations.

Elemental Analysis and IR Absorption Characterization. As used previously by Muetterties,[11] the analysis of the solid material has been obtained through elemental analysis. Results (Table S1) indicate that complexes with the ML_4 formula have been isolated. All the complexes have been found to have K^+ cation as counterion for the $[Ln(Trop)_4]^-$ anion.

The IR absorption spectra of tropolone, tropolonate (as potassium salt), and all the lanthanide complexes were recorded. The results are summarized in the Table S1. The H-bonded OH stretching vibration of tropolone is assigned to the broad band located between 3200 and 2500 cm^{-1}. This band is not present in the spectra of the potassium tropolonate and lanthanide complexes, providing a strong indication of a complete deprotonation of the OH group. The band around 1620 cm^{-1} present in the tropolone spectrum was assigned to the C═O bond stretching band. Upon deprotonation, this stretching band shifts to lower energy by 13 cm^{-1}. This change can be explained by the resonance of the deprotonated tropolonate anion (Scheme 1) which gives the C═O bond the mixed character of single and double bonds, therefore decreasing the stretching energy. Upon coordination, this vibration red-shifts by an additional 10 cm^{-1} due to a further decrease of the double bond character described above, which indicates that the oxygen atom of carbonyl group is involved in the complexation of Ln^{3+}. The stretching vibrations of C−O in tropolone disappear in potassium tropolonate and lanthanide complexes because the two CO vibrations are equivalent by resonance. Crystallography data also substantiate the equivalency of these two bonds (vide infra). The bond length of C═O in tropolone is 1.261 Å. In the complexes, the average CO bond length is longer (1.278(4) Å). A similar effect was observed for the C═C stretching vibration, which appears at 1542, 1530, and 1508 cm^{-1} in tropolone, potassium tropolonate, and lanthanide tropolonate, respectively.

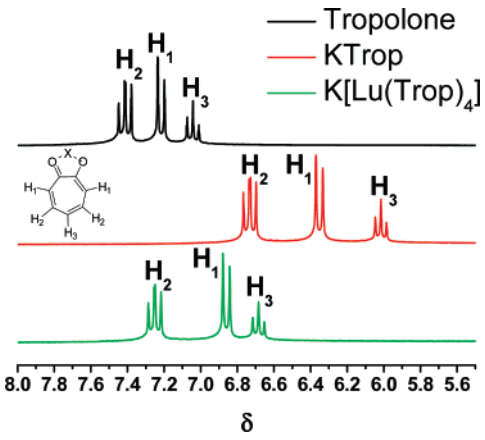

Figure 1. ^1H NMR spectra of tropolone, KTrop and K$[Lu(Trop)_4]$ at 298 K in DMSO-d_6.

The IR absorption bands of the troplone ligand located at 1241 and 711 cm^{-1} result from the in-plane and out-of-plane vibrations of C−H bonds, respectively.[28,29] Upon deprotonation and complexation, these C−H vibrations shift. These changes could be attributed to the change in rigidity of the tropolone ring upon coordination. The metal−oxygen bond vibration was identified in the IR spectra around 480−500 cm^{-1}. The frequency of this bond is an indication of the covalency of the M−O bond and has a higher value for heavier lanthanide ions.[30−32] This result is consistent with the previous study for lanthanide benzoates[33] and lanthanide 8-hydroxyquinoline complexes[34] for which an increase in covalency of the M−O bond in the heavier lanthanides identified by IR spectroscopy were also described.

NMR Analysis. The ^1H NMR spectra of tropolone, potassium tropolonate, and the diamagnetic Lu^{3+} complex K$[Lu(Trop)_4]$ were measured in DMSO-d_6. The chemical shift data are given in Table S2, and the ^1H NMR spectra are shown in Figure 1.

Due to the strong intramolecular hydrogen bonds present in tropolone, the proton from the OH group appears as a broad band with a chemical shift of 10.2 ppm (not shown in

(28) Selbin, J.; Ortego, J. D. *J. Inorg. Nucl. Chem.* **1968**, *30*, 313.
(29) Bagnall, K. W.; Bhandari, A. M.; Brown, D.; Lidster, P. E.; Whittaker, B. *J. Chem. Soc., Dalton Trans.* **1975**, 1249.
(30) Bünzli, J.-C. G.; Klein, B.; Pradervand, G. O.; Porcher, P. *Inorg. Chem.* **1983**, *22*, 3763.
(31) Bünzli, J.-C. G.; Mabillard, C.; Yersin, J. R. *Inorg. Chem.* **1982**, *21*, 4214.
(32) Bünzli, J.-C. G.; Yersin, J. R.; Mabillard, C. *Inorg. Chem.* **1982**, *21*, 1471.
(33) Taylor, M. D.; Carter, C. P.; Wynter, C. I. *J. Inorg. Nucl. Chem.* **1968**, *30*, 1503.
(34) Aly, H. F.; Abdel Kerim, F. M.; Kandil, A. T. *J. Inorg. Nucl. Chem.* **1971**, *33*, 4340.

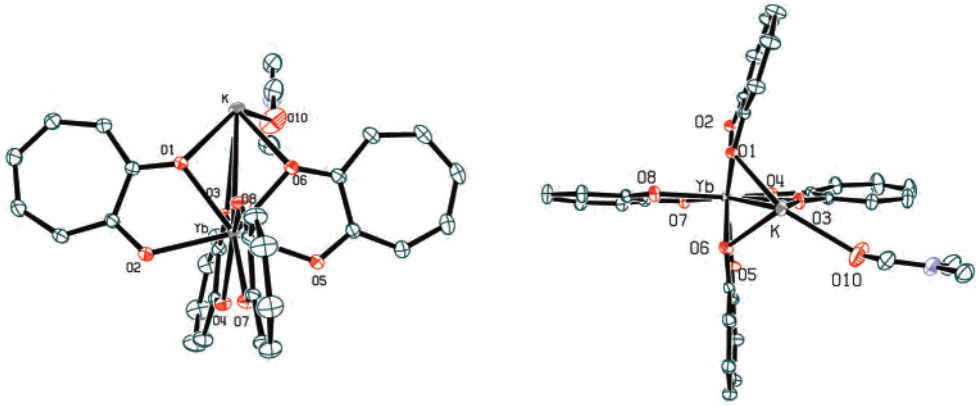

Figure 2. ORTEP representations of the molecular structure of {K[Yb(Trop)$_4$]DMF}$_\infty$ (50% probability ellipsoids, H atoms have been omitted for clarity).

Table 1. Summary of Crystal Data for {K[Ln(Trop)$_4$]DMF}$_\infty$ (Ln = Tb, Dy, Ho, Er, Tm, Yb, Lu)

complex	$C_{31}H_{27}O_9KTb$	$C_{31}H_{27}O_9DyK$	$C_{31}H_{27}O_9KHo$	$C_{31}H_{27}O_9ErK$	$C_{31}H_{27}O_9KTm$	$C_{31}H_{27}O_9KYb$	$C_{31}H_{27}O_9KLu$
M	755.56	759.14	761.57	763.90	765.57	769.68	771.61
space group	$P2_1/n$	$P\bar{1}$	$P\bar{1}$	$P\bar{1}$	$P\bar{1}$	$P\bar{1}$	$P\bar{1}$
a (Å)	12.7566(12)	7.3048(5)	7.2622(4)	7.2758(10)	7.296(3)	7.2409(3)	7.2465(4)
b (Å)	13.2771(12)	11.0879(8)	10.9440(6)	10.9867(16)	11.077(4)	10.9079(4)	10.9035(5)
c (Å)	18.9393(18)	20.1174(15)	19.9951(12)	20.037(3)	20.107(7)	19.8683(7)	19.8822(10)
α (deg)	90.00	79.3790(10)	80.0340(10)	79.993(3)	79.576(6)	80.0870(10)	80.1350(10)
β (deg)	95.984(2)	84.2300(10)	84.0010(10)	84.103(3)	84.340(7)	84.1570(10)	84.1030(10)
γ (deg)	90.00	78.8070(10)	78.8730(10)	78.941(3)	78.757(6)	78.8690(10)	78.8180(10)
V(Å^3)	3190.3(5)	1567.48(19)	1531.60(15)	1544.1(4)	1564.2(10)	1512.93(10)	1514.40(13)
Z	4	2	2	2	2	2	2
μ/mm^{-1}	2.399	2.569	2.773	2.906	3.022	3.283	3.452
T/K	295(2)	295(2)	150(2)	150(2)	150(2)	100(2)	150(2)
data collection range, θ/deg	1.84−32.53	1.90−32.51	1.92−32.47	2.03−32.58	2.01−25.00	1.93−32.52	1.93−32.49
reflns collected	40 368	20 601	13 209	19 971	11 424	19 668	19 694
independent reflns (R_{int})	11 227 (0.0588)	10 708 (0.0531)	9463 (0.0211)	10 444 (0.0246)	5128 (0.0152)	10 293 (0.0140)	10 268 (0.0577)
data/params	11 227/388	10 708/388	9463/388	10 444/472	5128/388	10 293/496	10 268/388
GOF on F^2	0.941	0.861	1.083	1.096	1.004	1.272	1.035
R1 [$I \geq 2\sigma(I)$][a]	0.0521	0.0342	0.0399	0.0276	0.0193	0.0209	0.0291
wR2[a]	0.1190	0.0666	0.0954	0.0660	0.0559	0.0544	0.0725

[a] $R1 = \sum||F_0| - |F_c||/\sum|F_0|$; $wR2 = \{\sum[w(|F_0|^2 - |F_c|^2|)^2]/\sum[w(F_0^4)]\}^{1/2}$.

Figure 1). After deprotonation, all the ring protons in tropolone shift to higher field. A similar effect was also observed by Poh et al. in a tropolone−triethylamine system.[35] When coordinated with Lu^{3+}, proton signals are shifted back to lower field because of the electron-withdrawing effect of Lu^{3+}, which decreases the electronic density on the protons.

Crystal Structure. X-ray quality crystals have been obtained for K[Ln(Trop)$_4$] with Ln = Tb, Dy, Ho, Er, Tm, Yb, Lu, allowing for a systematic analysis of the structure of the complexes and of the coordination geometry around the different lanthanide cations of the series. There are few reported examples of crystallographically characterized lanthanide complexes formed with the same ligand with a series of lanthanide cations. Of those few are the Ce^{3+}, Pr^{3+}, Nd^{3+}, Gd^{3+}, and Yb^{3+} complexes of the heptadentate ligand 2,2′,2″-tris(salicylideneimino)triethylamine.[36,37]

The crystallographic data for the tropolonate complexes are summarized in Table 1. With the exception of the Tb^{3+} complex, all the crystal structures are isomorphous. The structure of the Yb^{3+} complex is shown in Figure 2 as an example. The first sphere of coordination around each lanthanide cation is similar for all the different complexes analyzed. Each lanthanide cation is coordinated by four bidentate tropolonate ligands, and the resulting coordination number is 8. The average Ln−O bond length in each of these complexes ranges from 2.31 to 2.37 Å, steadily decreasing from Tb^{3+} to Lu^{3+} (Figure 3), which can be explained by the decrease in the respective effective ionic radii of the central lanthanide ion (1.04 Å for Tb^{3+} and 0.977 Å for Lu^{3+}, values obtained using Shannon[38] calculations for a coordination number of 8). The counterion K^+ bridges two $[Ln(Trop)_4]^-$ units being coordinated by six oxygen atoms, three from each unit of the complex, with an average K−O bond length of 2.8(1) Å. In addition, a DMF solvent molecule is coordinated to the K^+ by its carbonyl oxygen atom, leading to a total coordination number of 7 for K^+ (Figure 4 and Figure S1). Through the bridging K^+ ions, coordination polymeric chains are formed in the solid state, which have {K[Ln(Trop)$_4$]DMF} as the smallest common motif for the

(35) Poh, B.-L.; Siow, H.-L. *Aust. J. Chem.* **1980**, *33*, 491.
(36) Bernhardt, P. V.; Flanagan, B. M.; Riley, M. J. *Aust. J. Chem.* **2000**, *53*, 229.
(37) Bernhardt, P. V.; Flanagan, B. M.; Riley, M. J. *Aust. J. Chem.* **2001**, *54*, 229.
(38) Shannon, R. D. *Acta Crystallogr., Sect. A* **1976**, *A32*, 751.

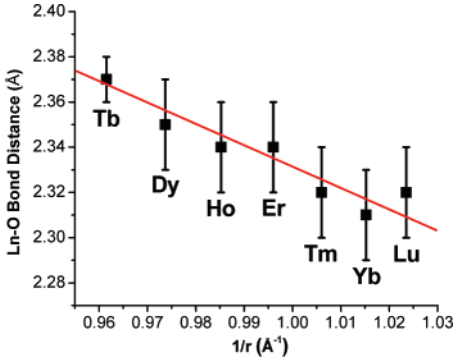

Figure 3. Ln−O bond length in $\{K[Ln(Trop)_4]DMF\}_\infty$ versus the reciprocal of the effective ionic radii (calculated according to Shannon for a coordination number of 8[38]).

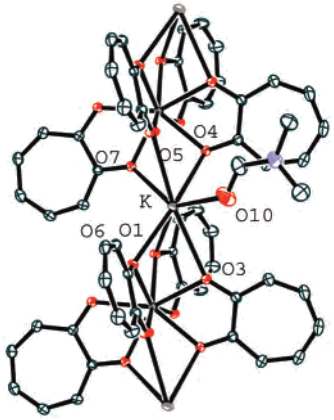

Figure 4. ORTEP representation of the coordination environment around K^+ in $\{K[Yb(Trop)_4]DMF\}_\infty$. (50% probability ellipsoids, H atoms have been omitted for clarity).

repeated unit. Figure 5 shows the polymeric chain of the complexes. The average distance between the closest Ln^{3+} and K^+ cations is fairly small at 3.88(2) Å (Table S3).

The main difference between the structure of the Tb^{3+} complex and the other ions are the relative positions of Ln^{3+} versus K^+ ions. The schematized views of the polymer chains for the two different types of complexes are presented in Figure 5. Although both polymer chains have a zigzag motif for the alternating Ln···K···Ln···K···Ln sequence, the two types of arrangements can be clearly distinguished by the relative position of K^+ with respect to the Ln···Ln···Ln sequence. In the structures of $\{K[Ln(Trop)_4]DMF\}_\infty$ (Ln = Dy−Lu), the K^+ ions are isotactic (on the same side of Ln···Ln···Ln), but in the Tb^{3+} complex, the K^+ ions are syndiotactic (located alternatively on both sides of Tb···Tb···Tb) (Figure 5). The difference of Ln···K···Ln···K···Ln sequences in the Tb^{3+} complex caused by the different packing mode of $[Ln(Trop)_4]^-$ units is probably due to the larger ionic radius of the Tb^{3+} cation.

Hydrogen Bonds and $\pi-\pi$ Stacking Interactions. Although C−H···O hydrogen bounds are typically weak interactions (<12 kJ/mol), they play an important role in supramolecular chemistry and crystal packing.[39] Several types of C−H···O hydrogen bonds have been identified for all seven crystal structures. Figure 6 illustrates the different types of hydrogen bonds observed in the Yb^{3+} (four types, see Table S4) and Tb^{3+} complexes (two types, see Table S4). The distances and angles between the donor and acceptor atoms are reported in Table S4 and are all in the range of typical C−H···O hydrogen bonds.[40]

$\pi-\pi$ stacking interactions are another type of weak interaction that can contribute to the crystal organization. There are typically two types of $\pi-\pi$ stacking interactions: face-to-face and slipped.[41] Both of them were identified in the complexes from Dy^{3+} to Lu^{3+} complexes. As an example, in the Ho^{3+} complex, the distance between the tropolone rings (C8−C14) in adjacent polymeric chains is 3.293 Å. The distance between the rings (C15−C21) is 3.695 Å. (Figure S2). Because the planes are crystallographically identical, the dihedral angles are zero. The distances in all of the complexes are listed in Table S3.

Geometry Analysis of the Complexes and of the Coordination around the Ln^{3+} Cations in the Solid State. Since seven crystal structures of the tropolonate complexes formed with different lanthanide cations were obtained, which has been rarely reported in the literature, we were able to collect a large amount of structural information on these complexes and to perform a systematic and comparative analysis of the coordination geometry around the lanthanide cations. In order to compare the tropolonate lanthanide complexes presented here with tropolonate complexes formed with other metal ions having a coordination number of 8, the Cambridge Structure Database (CSD) was searched and six structures were identified with the coordination motif $[M(Trop)_4]$ (M = Zr^{4+}, Nb^{5+}, Hf^{4+}, Sn^{4+}, Sc^{3+}).[42−47]

Evaluation of the geometry of these complexes was divided into two steps. First, the coordination polyhedron around the metal cation was identified using the analysis method from Kepert. Second, the deviation of the experimental coordination polyhedron from the ideal polyhedron was quantified.

Crystallographic data show that the coordination number of the central cation in all the analyzed tropolonate lanthanide complexes is 8. A typical example of the coordination polyhedron around Ln^{3+} in $K[Ln(Trop)_4]$ is depicted in Figure 7. Two different types of ideal coordination polyhedrons have a minimal energy for this coordination number: square antiprism (D_{4d}) and dodecahedron (D_{2d}). For coordination complexes formed with four bidentate ligands, the normalized bite (b) value is used as quantitative criteria to attribute if the coordination geometry around the lanthanide cation is closer to a square antiprismatic or to a dodecahedral

(39) Desiraju, G. R. *Acc. Chem. Res.* **1996**, *29*, 441.
(40) Jeffrey, G. A.; Maluszynska, H.; Mitra, J. *Int. J. Biol. Macromol.* **1985**, *7*, 336.
(41) Janiak, C. *Dalton Trans.* **2000**, 3885.
(42) Anderson, T. J.; Neuman, M. A.; Melson, G. A. *Inorg. Chem.* **1974**, *13*, 1884.
(43) Davis, A. R.; Einstein, F. W. B. *Inorg. Chem.* **1974**, *13*, 1880.
(44) Davis, A. R.; Einstein, F. W. B. *Acta Crystallogr., Sect. B* **1978**, *B34*, 2110.
(45) Tranqui, D.; Tissier, A.; Laugier, J.; Boyer, P. *Acta Crystallogr., Sect. B* **1977**, *B33*, 392.
(46) Kira, M.; Zhang, L. C.; Kabuto, C.; Sakurai, H. *Organometallics* **1998**, *17*, 887.
(47) Davis, A. R.; Einstein, F. W. B. *Inorg. Chem.* **1975**, *14*, 3030.

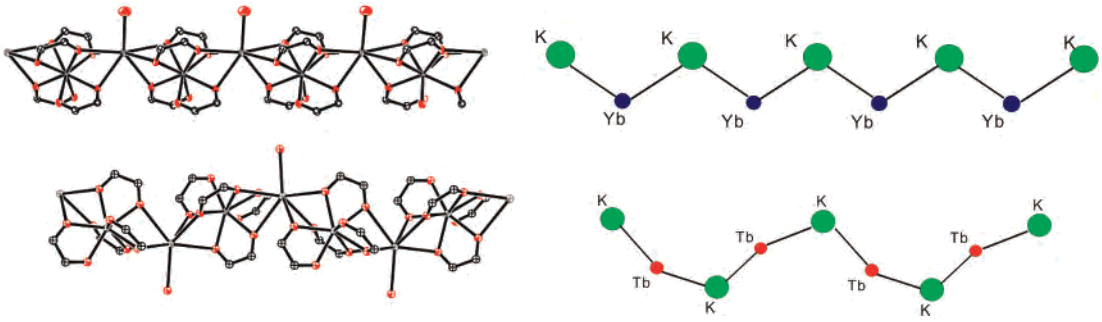

Figure 5. Representation of the polymeric chain in $\{K[Yb(Trop)_4]DMF\}_\infty$ (top) and $\{K[Tb(Trop)_4]DMF\}_\infty$ (bottom).

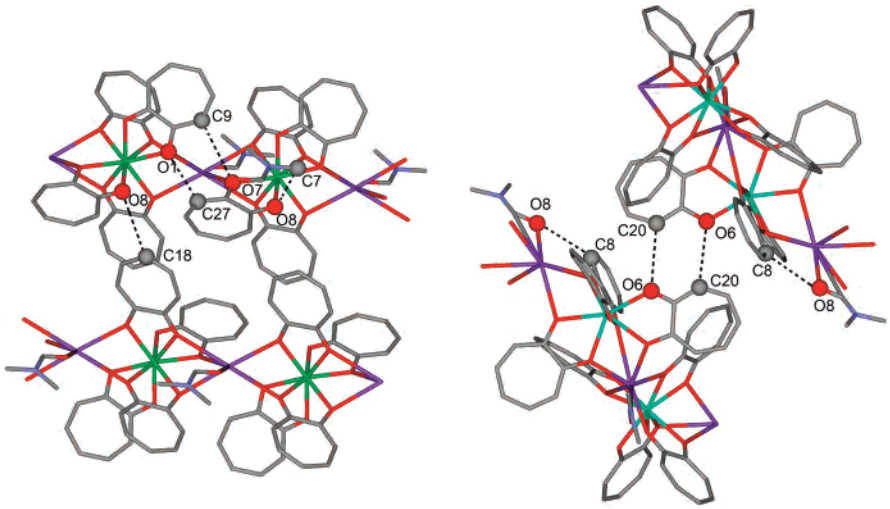

Figure 6. C−H···O hydrogen bonds in $\{K[Yb(Trop)_4]DMF\}_\infty$ (left) and $\{K[Tb(Trop)_4]DMF\}_\infty$ (right).

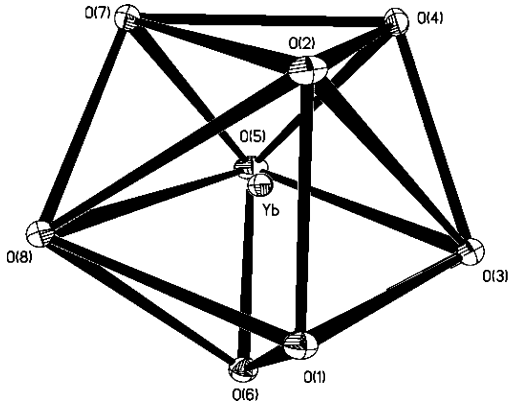

Figure 7. Coordination polyhedron around Yb^{3+} in $[Yb(Trop)_4]^-$ as obtained from X-ray crystallographic data.

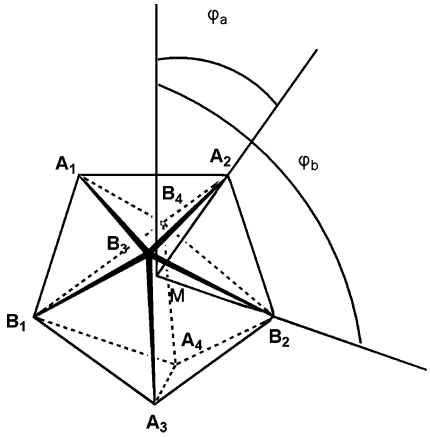

Figure 8. Dodecahedron model for the geometrical analysis.

coordination geometry. Empirical relationships between the coordination geometry of tetra-bidentate complexes and their normalized bite have been put forth by Kepert.[48] The normalized bite is defined as the ratio of the distance of the two oxygen atoms in the bidentate ligands (d_{O-O}) to the bond length of M−O (d_{M-O}): d_{O-O}/d_{M-O}. Complexes with $b < 1.1$ are classified as adopting D_{2d} dodecahedral coordination geometries, where complexes with b values comprised between 1.15 and 1.20 possess intermediate D_2 stereochemistries. Complexes formed with bidentate ligands with $b > 1.3$ can be classified as having D_4 square antiprismatic coordination geometries. A theoretical model of a dodecahedron is represented in Figure 8. The results of these calculations for the tropolonate complexes formed with both lanthanide cations (this work) and other metal ions are reported in Table 2. All the lanthanide tropolonate complexes presented here have b values between 1.07 and 1.10, which allows us to conclude, according to the Kepert criteria, that all lanthanide complexes for which a crystal structure has been obtained adopt D_{2d} dodecahedral coordination geometries. For the other six tropolonate complexes formed with other metal ions, the b values fall within 1.12−1.17 and indicate the D_2 intermediate stereochemistries. In the existing literature, the coordination polyhedra observed for the Nb^{5+}

(48) Kepert, D. L. *Prog. Inorg. Chem.* **1978**, *24*, 179.

Table 2. Results of Geometrical Analysis of Dodecahedra in the Different Complexes

	Tb	Dy	Ho	Er	Tm	Yb	Lu	Sc1[42]	Sc2[43]	Zr[44]	Hf[45]	Sn[46]	Nb[47]	ideal dodecahedron
φ_a (deg)[a]	36	39	39	39	39	39	39	36	36	37	36	36	36	35.2
φ_b (deg)[a]	101	104	105	105	105	106	105	105	105	105	106	107	106	106.5
a[b]	1.00	0.99	1.00	0.99	0.99	0.99	0.99	1.00	1.00	1.01	1.00	1.01	1.00	1.03
θ (deg)[c]	178	172	172	172	173	173	173	172	172	173	179	178	178	180
ω_i (deg)[d]	0	3	3	3	9	21	3	18	9	1	2	6	4	0
	2	1	1	1	2	10	2	11	15	2	5	7	5	0
	6	7	17	5	2	2	6	6	6	3	2	20	10	0
	3	19	6	3	5	1	12	8	9	1	2	19	10	0
d_{O-O} (Å)	2.54	2.55	2.56	2.56	2.55	2.54	2.55	2.50	2.50	2.46	2.49	2.55	2.43	
d_{M-O} (Å)	2.37	2.35	2.34	2.34	2.32	2.31	2.32	2.21	2.21	2.18	2.18	2.17	2.09	
b[e]	1.07	1.08	1.09	1.09	1.10	1.10	1.10	1.13	1.13	1.12	1.14	1.17	1.16	
r_M (Å)[f]	1.04	1.027	1.015	1.004	0.994	0.985	0.977	0.87	0.87	0.84	0.83	0.81	0.74	

[a] φ_a and φ_b are the average values of the angles between $\mathbf{R_1}$-$\mathbf{R_2}$ and A_i (i = 1, 2, 3, 4) and B_i (i = 1,2 3,4), respectively. The error in the angles is typically 1°. [b] a is the ratio of the bond length |M−A| to |M−B|. [c] θ is the angle between $\mathbf{R_1}$ and $\mathbf{R_2}$. [d] ω_i are the angles between the **Ln-O** vectors belonging to the same tropolonate ligand. [e] b is the ratio between d_{O-O} and d_{M-O}. [f] r_M is the effective ionic radii (calculated according to Shannon for a coordination number 8[38]).

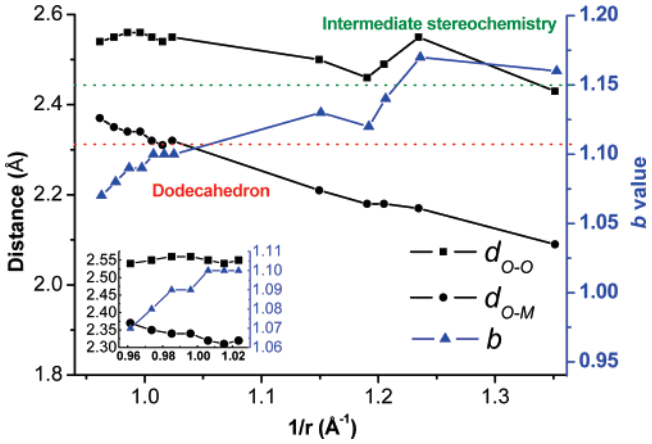

Figure 9. Average distances between oxygen atoms in tropolonate ligand, M−O bond lengths, and normalized bite b values for different tropolonate complexes.

and Sn^{4+} complexes were assigned to an irregular bicapped trigonal prism distorted toward a dodecahedron by their authors.[46,47]

It can be observed from the comparison of the d_{O-O}, d_{M-O}, and b values, reported in Table 2 and shown in Figure 9, that there is an almost monotonous linear relationship between the d_{M-O} distances and the sizes of the metal cations; the smaller the size of central metal ion, the shorter the d_{M-O} distance. The relationship between the oxygen−oxygen distances, d_{O-O}, and the size of the metal ions adopts two different regimes for lanthanide and for the other metal ions. This relationship is almost linear for the lanthanide cations. Two important changes in slopes are observed for the other ions with two abrupt changes, the slope is strongly positive from Zr^{4+} to Sn^{4+} and becomes negative from Sn^{4+} to Nb^{5+} (Figure 9). This indicates that parameters that control the coordination geometry around metal cations are significantly different for lanthanide and other metal ions, even if they form the same type of complexes with tropolonate ligands with the same coordination numbers. This is attributed to the difference in the nature of the orbitals of these metal ions.

We have demonstrated that, according to the Kepert definition, for all the ML_4 *lanthanide* tropolonate complexes for which crystal structures have been isolated, the central cations adopt a dodecahedral coordination geometry. A shape analysis was undertaken to quantify the level of distortion from the ideal coordination polyhedron. For each lanthanide complex analyzed, the coordination sphere around the cation has been analyzed using geometrical considerations assuming that the S_4 improper axis of rotation was maintained for all the complexes formed (Figure 10). Three parameters are relevant to confirm the dodecahedral shape: (i) the angle between $\mathbf{R_{M-A}}$ (vector of the M−A bond) and the S_4 axis (φ_a), (ii) the angle between $\mathbf{R_{M-B}}$ (vector of the M−B bond) and the S_4 axis (φ_b), and (iii) the ratio, a, between bond length |M−A| and |M−B|. For an ideal dodecahedron, these three theoretical values are 35.2°, 106.5°, and 1.03, respectively. To quantify the presence of the pseudo-S_4 improper rotation axis, the sum of vectors $M-A_1$, $M-A_2$, $M-B_3$, and $M-B_4$ was defined as vector $\mathbf{R_1}$, the sum of vectors $M-B_1$, $M-B_2$, $M-A_3$, and $M-A_4$ was defined as vector $\mathbf{R_2}$, and the vector $\mathbf{R_1}$-$\mathbf{R_2}$ is defined as the pseudo-S_4 axis (Figure 10). The angle between $\mathbf{R_1}$ and $\mathbf{R_2}$ is defined as θ. The projections of Ln and the eight oxygen atoms of the coordination sphere onto a plane perpendicular to the $\mathbf{R_1}$-$\mathbf{R_2}$ direction were then calculated. The angle, ω_i, located between the vectors Ln−O belonging to the same ligand (**Ln-A$_i$** and **Ln-B$_i$**) is the direct quantification of the deformation of the pseudo-dodecahedron from its ideal geometry (ideal $\omega = 0°$). The assignments for the oxygen atom present in different complexes are shown in Table S5. The values for φ, θ, and ω_i are reported in Table 3.

It can be concluded from this treatment of the experimental data that the geometries of coordination polyhedra in the tropolonate lanthanide complexes possess some distortion relative to the ideal dodecahedron. This could be explained by the shape of the molecule in the crystal packing, which is affected by the presence of K^+ and the DMF solvent molecule. In the crystals, K^+ is coordinated to the oxygen atoms in the deprotonated tropolonate ligands and the DMF is coordinated to K^+ (see above). This induces one of the tropolonate planes to deviate significantly from its ideal position, and as a consequence, two of the four dihedral

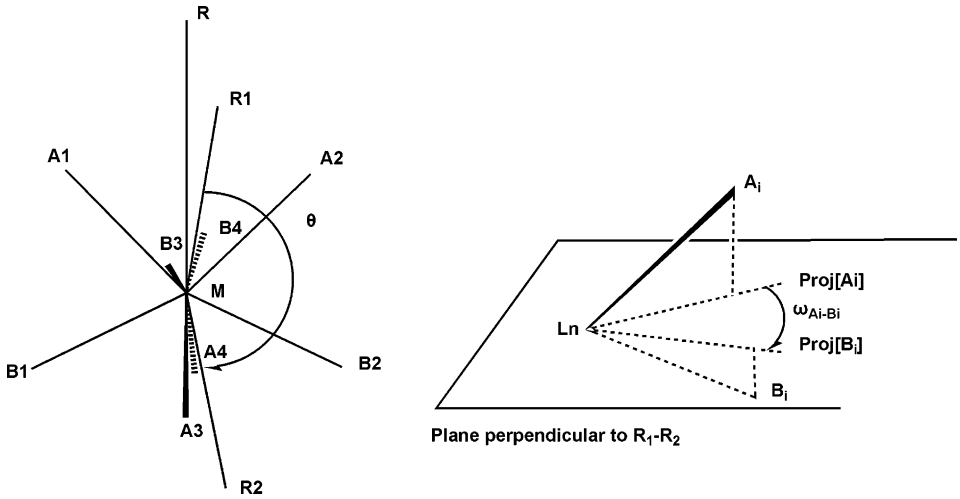

Figure 10. Definition of the angles and vectors used in the geometrical analysis.

Table 3. Calculated Formation Constants for ML_3 and ML_4 Complexes

	La	Nd	Sm	Gd	Ho	Er	Yb	Lu
log K_3	5.6(3)	5.7(3)	5.7(3)	5.6(3)	6.0(3)	5.9(3)	6.0(3)	6.1(3)
log K_4	4.8(3)	4.8(3)	4.5(3)	4.7(3)	4.8(3)	4.8(3)	4.4(3)	4.5(3)

angles deviate from the ideal values of 90°, one of the dihedral angles being larger and the other one being smaller (Table S6).

Solution Behavior. In order to compare the tropolonate lanthanide complexes formed in solution and in the solid state, the compounds were analyzed and compared using different techniques.

ESI-MS. Electrospray ionization mass spectra (ESI-MS) were recorded for all the different lanthanide complexes (Ln = La, Pr, Nd, Sm, Eu, Gd, Tb, Dy, Ho, Er, Tm, Yb, Lu) in a mixture of DMF and methanol solution. They all show rather similar peak patterns in both positive and negative spectra. Typical examples of spectra are depicted in Figure 11. The detailed results are listed in Table S7. Selected spectra for the different species are shown in Figure S3. In the negative ion mode spectra, the presence of the $[Ln(Trop)_4]^-$ peak (Figure 11) indicate the formation of ML_4 complex in solution. Other peaks were also observed on the spectra such as the free tropolonate anion with a lower abundance whose presence can be attributed to the partial dissociation of the ML_4 complex in the chosen experimental conditions. It is important to notice that the ML_3 species cannot be detected in this experiment because it is not ionized. In the positive ion mode spectra, several types of ions were observed: $[Ln(Trop)_2]^+$, $[Ln(Trop)_2+DMF]^+$, $[Ln(Trop)_3+Na]^+$, $[Ln(Trop)_3+K]^+$, $[Ln(Trop)_4+2Na]^+$, $[Ln(Trop)_4+Na+K]^+$, and $[Ln(Trop)_4+2K]^+$. In addition, the signal of di- and trinuclear species such as $[Ln_2(Trop)_5]^+$, $[Ln_2(Trop)_6+Na]^+$, $[Ln_2(Trop)_6+K]^+$, $[Ln_3(Trop)_8]^+$, $[Ln_3(Trop)_9+Na]^+$, and $[Ln_3(Trop)_9+K]^+$ were also detected. This may indicate that there is significant interaction between the $Ln(Trop)_n$ units when the $K[Ln(Trop)_4]$ complex is present at high concentration (10^{-3} mol/L). Other phenomena such as fragmentation, ligand exchange, and clustering reactions during the mass spectral experiments could also account for the diverse ionic species observed. Tedeschi et al.[49] also observed a polynuclear pattern of peaks in ESI-MS with the 1,2-HOPO lanthanide complexes that they studied. Analysis obtained from spectrophotometric titrations (vide infra) did not indicate the presence of di- and trinuclear species.

Spectrophotometric Titration. To determine the number and nature of species formed in solution and the corresponding stability constants for the lanthanide tropolonate complexes, spectrophotometric titrations were performed for La^{3+}, Nd^{3+}, Sm^{3+}, Gd^{3+}, Ho^{3+}, Er^{3+}, Yb^{3+}, and Lu^{3+}. A typical example of experimental data for the titration of the Yb^{3+} complex is depicted in Figure 12. In this experiment, the lanthanide salt is added to a solution of deprotonated ligand (potassium tropolonate).

Factor analysis indicated the presence of five independent colored species in the solution. For each lanthanide cation, experimental data were successfully fitted with a model where four complexes are successfully formed in solution: ML, ML_2, ML_3, and ML_4 (this model is compatible with the factor analysis results). Stability constants for ML_3 and ML_4 were obtained on the basis of this model (Table 3) at the condition of fixing the values of log K_1 and log K_2 to values larger than 9.[50] This can be explained by the relatively high stability of the ML_1 and ML_2 complexes in solution. At the concentrations in which the experiments were conducted, insufficient information on these species is present to allow for accurate calculation with the Specfit software.

The calculated formation constant of ML_3 and ML_4 shows different trends that depend on the size of lanthanide cations (Figure 13). log K_3 increases as the size of the lanthanide decreases. This is the typical trend observed for lanthanide cations where no steric hindrance is present between ligands upon complex formation, as the interaction between lanthanide cations and the ligand is mainly electrostatic.[50] The strength of this interaction increases with the atomic number of the lanthanide. As the atomic number increases, the charge density on the lanthanide cation increases, leading to larger

(49) Tedeschi, C.; Azema, J.; Gornitzka, H.; Tisnes, P.; Picard, C. *Dalton Trans.* **2003**, 1738.
(50) Petoud, S.; Bünzli, J.-C. G.; Renaud, F.; Piguet, C.; Schenk, K. J.; Hopfgartner, G. *Inorg. Chem.* **1997**, *36*, 5750.

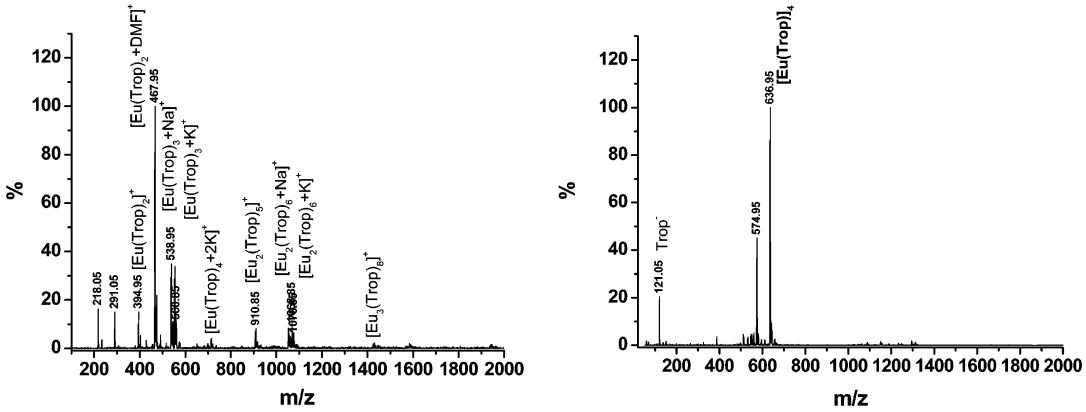

Figure 11. ESI-MS spectra for K[Eu(Trop)$_4$].

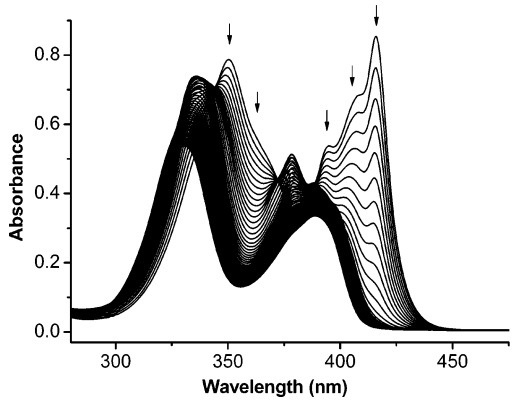

Figure 12. Example of absorption spectra collected during a spectrophotometric titration of the tropolonate ligand solution with Yb^{3+} in DMSO (total ligand concentration: $\sim 5 \times 10^{-5}$ mol/L; aliquots of $YbCl_3$ in DMSO were successively added (up to 1:1 metal/ligand ratio); $T = 25.0 \pm 0.1$ °C; 0.01 M tetrabutylammonium perchlorate for ionic strength control, arrows indicate continuous changes in signal (upon lanthanide addition).

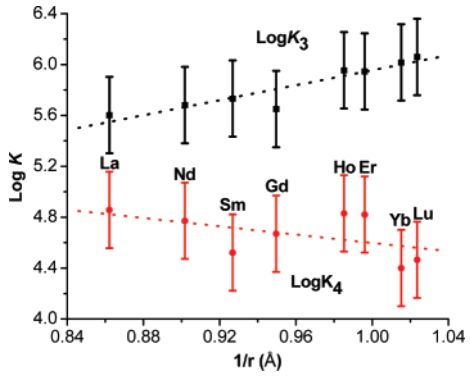

Figure 13. Plot of the calculated values of log K_3 and log K_4 obtained from the analysis of the experimental data with Specfit versus the reciprocal of the size of the effective ionic radii of the lanthanide cations calculated according to Shannon.[38]

log K_3 values. log K_4 values for the different lanthanides of the series show a different trend by steadily decreasing as the size of the lanthanide cation decreases. This can be explained by the steric hindrance generated between the four ligands when ML_4 is formed. This steric hindrance increases with smaller lanthanide cations since the ligands must be located at closer proximity when the lanthanide cations' effective radii decrease.

Unlike preorganized tridentate ligands such as substituted bis(benzimidazolyl)pyridines[50] and N_4O_3 tripodal amine phenol ligands,[51] bidentate tropolonate ligands do not induce a size-discrimination effect (size selectivity) based on the size of the lanthanide cation upon formation of the ML_4 complexes. This can be explained by the lack of ligand preorganization. For example, three bis(benzimidazolyl)-pyridine ligands[50] form ML_3 complexes with lanthanides wrapping around the central cation and forming a cavity with a specific size to accommodate the lanthanide cation. Tropolonate is only a bidentate ligand with a lower level of preorganization, which may explain the steady decrease of the stability with the decrease of the size of the metal ion instead of observing a peak of size selectivity.

In summary, these measurements have demonstrated that the tropolonate ligands react with all the lanthanide cations of the series to form ML_1, ML_2, ML_3, and ML_4 complexes successively. The ML_4 species that has been observed in the solid sate from the X-ray diffraction experiments is also formed in solution under specific conditions (mainly stoichiometry and concentration).

Protection of the Lanthanide Cations in the Solid State and in Solution. Information on the structure of $[Ln(Trop)_4]^-$ obtained on the basis of the crystal structure data indicate that, in the solid state, lanthanide cations are coordinated with four tropolonate ligands and are well protected from solvent molecules since none were detected in the first coordination sphere of the lanthanide cation. To evaluate the situation in solution, Ln^{3+}-centered luminescence lifetimes measured upon ligand excitation have been recorded in different solvents in order to determine the nature of the coordination environment around the lanthanide cation when the $[Ln(Trop)]_4^-$ complex is in solution.

The hydration state of lanthanide ion in a coordination complex can be estimated by using an empirical formula (eq 1) developed by Horrocks et al.,[52,53] where q is the number of the water molecules bound to the lanthanide ion and k_{H2O} and k_{D2O} are the rate constants of the excited states of the lanthanide ion in H_2O and D_2O, respectively. A is a proportionality constant related to the sensitivity of the lanthanide ion to vibronic quenching by OH oscillators.

(51) Caravan, P.; Hedlund, T.; Liu, S.; Sjöberg, S.; Orvig, C. *J. Am. Chem. Soc.* **1995**, *117*, 11230.
(52) Horrocks, W. D., Jr.; Sudnick, D. R. *J. Am. Chem. Soc.* **1979**, *101*, 334.
(53) Horrocks, W. D., Jr.; Sudnick, D. R. *Acc. Chem. Res.* **1981**, *14*, 384.

Beeby et al. revised it to eq 2 for Eu^{3+}, Tb^{3+}, and Yb^{3+}-complexes in water, where the outer-sphere quenchers are taken into account by adding a correction factor, *B*.[54]

$$q = A(k_{H2O} - k_{D2O}) \quad (1)$$

$$q = A(k_{H2O} - k_{D2O}) - B \quad (2)$$

More recently, Davies et al.[55] and Beeby et al.[56] modified this formula for the determination of *q* for Yb^{3+} and Nd^{3+} complexes in MeOH solutions, respectively.

For the Yb^{3+} complex

$$q = k_{H2O} - k_{D2O} - 0.1 = 1/\tau_{H2O} - 1/\tau_{D2O} - 0.1 \quad (3)$$

$$q = 2(k_{CH3OH} - k_{CD3OD}) - 0.1 = 2(1/\tau_{CH3OH} - 1/\tau_{CD3OD}) - 0.1 \quad (4)$$

(All the rate constants are expressed in units of μs.)

Applying these formulas for the tropolonate Yb^{3+} complex, *q* values were calculated as 1.13 in water ($\tau_{H2O} = 0.75 \pm 0.01$ μs, $\tau_{D2O} = 10.0 \pm 0.1$ μs) and 0.98 in methanol ($\tau_{CH3OH} = 1.62 \pm 0.03$ μs, $\tau_{CD3OD} = 13.02 \pm 0.01$ μs). Due to the limited solubility of these complexes in methanol and water, they were dissolved in a mixture of DMSO (5% by volume) and methanol or water, respectively. These values consistently indicate that in both types of solvents, one water molecule is bound to the lanthanide ion in the first sphere of coordination. The structure in solution therefore has to be different from the structure observed in the solid state, where no coordinated solvent molecules were present in the first coordination sphere. The four tropolonate ligands in $[Ln(Trop)_4]^-$ do not efficiently protect the Ln^{3+} cation from nonradiative deactivations induced by coordinated water molecules in solution. This system of coordination complexes is an example where the structure observed in the solid state does not reflect the structure of the complex in solution.

Conclusion

In this paper, the structures of ML_4 complexes formed between tropolonate ligands and lanthanide cations in the solid state were systematically studied and compared. It was observed that for each of the lanthanide complexes analyzed ($Ln^{3+} = Tb^{3+}$, Dy^{3+}, Ho^{3+}, Er^{3+}, Tm^{3+}, Yb^{3+}, Lu^{3+}), four tropolonate ligands coordinate to one lanthanide cation, the coordination number around the lanthanide cation being 8 and the coordination polyhedron being best described as a slightly distorted dodecahedron. The systematic analysis of the experimental data obtained from the X-ray crystal structures shows that the coordination geometries around the different lanthanide cations are similar for all the different complexes.

The crystal packing of the molecules was similar for $Ln^{3+} = Dy^{3+}$, Ho^{3+}, Er^{3+}, Tm^{3+}, Yb^{3+}, Lu^{3+}. A change in the packing mode of the molecules in the crystal has been observed for the largest lanthanide cation of our series (Tb^{3+}). We explain this change by the increase in size of the lanthanide cation which generates a modification in the coordination mode of the potassium counterion and in the resulting crystal packing of the molecules.

In solution, spectrophotometric titrations confirmed that the ML_1, ML_2, ML_3, and ML_4 species are successively formed in solution. The stability constant values of the ML_3 complexes increase as the lanthanide cation's radius decrease. This behavior has been typically observed for complexes where bonds are mainly of electrostatic nature. However, this situation is quite different for the ML_4 complexes, where the stability constant values of ML_4 steadily decrease as the lanthanide's size decreases. This can be explained by the steric hindrance generated by the four tropolonate ligands around the lanthanide cation upon formation of the ML_4 complex.

Luminescence lifetimes of the Yb^{3+} complex in H_2O/D_2O and MeOH/MeOH-d_4 indicate that the coordination geometries around the Ln^{3+} cation in the ML_4 complexes in solution are different than those in the solid state. These measurements provide evidence of the presence of one water (methanol) molecule in the first coordination sphere. However, no solvent molecule was observed as being bound to the lanthanide cation in the crystal structure. This demonstrates that coordination chemists must be careful in using X-ray data to explain the solution behavior of coordination complexes.

Acknowledgment. Funding was provided through the University of Pittsburgh and through the National Science Foundation (Award No. DBI 0352346). Jian Zhang was supported through an Andrew Mellon Predoctoral Fellowship.

Supporting Information Available: ^{1}H NMR, elemental analysis, and IR data, additional structural information, and mass spectrometry data. This material is available free of charge via the Internet at http://pubs.acs.org.

IC7005343

(54) Beeby, A.; Clarkson, I. M.; Dickins, R. S.; Faulkner, S.; Parker, D.; Royle, L.; de Sousa, A. S.; Williams, J. A. G.; Woods, M. *J. Chem. Soc., Perkin Trans. 2* **1999**, 493.
(55) Davies, G. M.; Aarons, R. J.; Motson, G. R.; Jeffery, J. C.; Adams, H.; Faulkner, S.; Ward, M. D. *Dalton Trans.* **2004**, 1136.
(56) Beeby, A.; Burton-Pye, B. P.; Faulkner, S.; Motson, G. R.; Jeffery, J. C.; McCleverty, J. A.; Ward, M. D. *J. Chem. Soc., Dalton Trans.* **2002**, 1923.